Cell. Mol. Life Sci. 66 (2009) 324 – 338
1420-682X/09/020324-15
DOI 10.1007/s00018-008-8424-4

Cellular and Molecular Life Sciences

Research Article

Src activation and translocation from focal adhesions to membrane ruffles contribute to formation of new adhesion sites

A. Hamadi, T. B. Deramaudt, K. Takeda and P. Rondé*

UMR CNRS 7175, Dépt. Pharmacologie et Physicochimie, Université Louis Pasteur – Strasbourg I, Faculté de Pharmacie, 74 rte du Rhin, BP 60024, 67401 Illkirch (France), Fax: +33 390 24 43 13,
e-mail: philippe.ronde@pharma.u-strasbg.fr

Received 21 July 2008; received after revision 10 October 2008; accepted 03 November 2008
Online First 10 December 2008

Abstract. Cell migration requires the coordinated turnover of focal adhesions, a process that involves FAK phosphorylation. Since Src is the major kinase implicated in FAK phosphorylation, we focus here on the role of Src activation on adhesion remodelling. In astrocytoma cells, constitutively activated Src induces both FAK phosphorylation and adhesion rearrangement. To evaluate how Src controls these processes, we used a recently described Src reporter to monitor the dynamics of Src phosphorylation. Upon Src activation, focal adhesions started to disassemble while Src appeared highly expressed at newly formed membrane ruffles. Kinetic analysis of time-lapse movies showed that loss of phospho-Src at focal adhesions was time-correlated with the appearance of membrane ruffles containing phospho-Src. Moreover, FLIP analysis revealed a dynamic equilibrium of Src between focal adhesions and membrane ruffles. We conclude that upon phosphorylation, Src is directly translocated from focal adhesions to membrane ruffles, thereby promoting formation of new adhesion complexes.

Keywords. Src, tyrosine phosphorylation, Src indicator, focal adhesion dynamics, FAK.

Introduction

The protein tyrosine kinase v-Src is the transforming product of Rous sarcoma virus, the first identified oncogenic retrovirus. Src, the cellular counterpart of v-Src, is a member of a multigene family of membrane-associated non-receptor tyrosine kinases known as SFKs [1] which also includes Fyn and Yes. Src is ubiquitously expressed in mammalian cells and is known to modulate the actin cytoskeleton and cell adhesion structures such as focal adhesions [2]. Focal adhesions consist of clustered integrins and proteins that link the extracellular matrix (ECM), through integrins, to the actin cytoskeleton and to proteins involved in adhesion-dependent signal transduction [3, 4]. The role of Src in focal adhesions is associated with cell detachment, migration and invasion, processes which are essential in the dissemination of cancer cells [5]. Specifically, Src-transformed cells display reduced numbers of bundled actin filaments and cellular contacts. For example, in primary chicken embryo fibroblasts, the temperature-sensitive LA29 v-Src protein induces a highly altered phenotype by completely disrupting all focal adhesions, resulting in cell rounding and, in extreme cases, cell detachment [6]. The importance of SFKs as regulators of cell spreading and cell migration is also highlighted by studies from knockout mice showing abnormalities in cell migration and adhesion. Indeed, fibroblasts from

* Corresponding author.

mice deficient in Src, Yes and Fyn display reduced motility and spreading, with the apparent rate constant for adhesion turn-over being decreased 19-fold in $SFK^{-/-}$ fibroblasts compared to wild-type fibroblasts [7].

SFK family members have the following common domains: a N-terminal region containing attachment sites for saturated fatty acid addition, a Src-homology 3 (SH3) domain, a Src-homology 2 (SH2) domain, a tyrosine kinase domain (SH1), and a C-terminal negative regulatory domain. In adhesion events, an important Src substrate is another non receptor tyrosine kinase called focal adhesion kinase (FAK; [8, 9]). Integrin binding to the extracellular matrix triggers phosphorylation of FAK at tyrosine 397, which is an autophosphorylation site [9–12]. Once phosphorylated, Tyr-397 generates a high affinity binding site for SH2 domain-containing proteins such as Src family kinases [9, 13, 14]. Src binding to FAK apparently contributes to Src activation, promoting further phosphorylation of FAK at additional tyrosines, namely Tyr-861 [15] and Tyr-925 [1, 16, 17]. This in turn is believed to be responsible for efficient FA disassembly and migration [1, 6, 18]. Indeed, studies using either specific inhibitors of Src such as PP2 and AP23464 or $SYF^{-/-}$ fibroblasts, together with studies using a kinase dead mutant of Src, reveal the essential role of the kinase domain of Src for both FAK phosphorylation and focal adhesion disassembly [1, 6, 7, 16, 19]. On the other hand, the SH2 domain of Src seems to be necessary for FAK-mediated Src targeting to focal adhesion sites [13, 16, 20] although other studies have implicated the SH3 domain of Src in both targeting Src to focal adhesion and enhancement of FAK phosphorylation [21, 22]. Moreover, this domain may support cell invasion by promoting the formation of a FAK/Src complex at β1-integrin-containing invadopodia [23].

Cell invasion was also linked to transient accumulation of FAK at lamellipodia with formation of a FAK/Src signalling complex [24]. On the other hand, Src was also shown to be localized at membrane ruffles, although the specific role of Src at these sites was not well established [25]. These data suggest a dynamic role for Src in the formation and dissociation of cellular structures implicated in cell migration and invasion. Indeed, it is well known that Src is implicated in actin rearrangement necessary for the remodelling of the cellular adhesion/cytoskeletal network [26–28]. For example, Src is absolutely required at peripheral cell-matrix attachment sites for the efficient conversion of focal adhesion into lamellipodia [29]. Nevertheless, the mechanism by which Src induces efficient remodelling of FAs into lamellipodia or filopodia is unclear. For example, it is not known whether activated Src is needed during the onset of FA disassembly and/or during the onset of lamellipodia formation. Moreover, the intracellular trafficking of Src during adhesion remodelling has never been clearly documented.

In this report, therefore, we investigated the spatio-temporal regulation of Src activity at peripheral adhesion sites. To characterize the activity of Src and its trafficking during adhesion remodelling, we used a phospho-reporter to monitor the behaviour of activated Src in living cells. We report here for the first time that increase in phosphorylation of Src induces translocation of Src from focal adhesions to membrane ruffles during the edge extension/retraction cycle.

Materials and methods

Reagents and antibodies. Eagle's minimum essential medium (EMEM), foetal bovine serum (FBS), ultra-glutamine, penicillin, streptomycin, and trypsin-EDTA solution were from BioWhittaker. Matrigel and mouse monoclonal antibody (Ab) directed against amino acids 354–533 of the FAK kinase domain (anti-FAK kinase) were from BD Biosciences. Anti-Y861-phospho-FAK (P-Y861) and anti-Y397-phospho-FAK (P-Y397) Abs were from BioSource International. Anti-Y925-phospho-FAK Ab was from US Biological. Anti-Src and anti-Y418-phospho-Src Abs were from Cell Signaling. The Src inhibitors PP2 and PP3 were from Calbiochem. Horseradish peroxidase-conjugated goat anti-mouse or anti-rabbit IgGs were from Promega. Anti-cortactin Ab was from Millipore. Phalloidin fluoProbe 547 was obtained from Interchim. Rhodamine Red X-conjugated goat anti-mouse or anti-rabbit Abs were from Jackson Labs. All transfections were done using Fugene 6 [25]. G418 sulfate was from Invitrogen. Pervanadate solution at 1 mM was freshly prepared by mixing vanadate solution (Sigma) and hydrogen peroxide in PBS to final concentrations of 1 mM and 0.006% respectively. A final concentration of 100 μM pervanadate was used to pretreat the cells.

Expression vectors. The pcDNA3 plasmid containing the Src Indicator (SrcI) was kindly provided by R.Y. Tsien. The pcDNA3 plasmid containing Src-Y530F was kindly provided by F. Cruzalegui. mRFP was expressed in pcDNA3 plasmid. All plasmids were verified by sequencing and isolated using the JetStar Plasmid kit (Genomed) following the manufacturer's protocol.

Cell culture and stable transfections. The U87-MG human astrocytoma cell line was obtained from the American Type Culture Collection. Cells were maintained in EMEM supplemented with 10% heat-inactivated FBS, 2 mM ultraglutamine, and 1 mg/ml G418. Cell lines were kept as subconfluent monolayers and were maintained in a 5% CO_2 humidified incubator at 37°C. For stable transfection, cells were plated 24 h in 6-well plates and then transfected using Fugene 6 according to the manufacturer's directions. After 48 h, transfected cells were selected in culture medium containing 1 mg/ml G418.

Immunoblotting. For Western blots, Src-Y530F or SrcI-expressing cells were plated at low density on dishes pre-coated with 178 μg/ml Matrigel and cultured for 2 d. Cells were then washed with cold PBS and lysed with RIPA buffer. Protein lysates were resolved by SDS-PAGE (8% polyacrylamide) and then transferred to polyvinylidene difluoride membranes (Amersham). After 1 h blocking at room temperature in 0.1% casein-PBST (PBS supplemented with 0.1% Tween 20), membranes were incubated overnight with primary Abs at 4°C: anti-Src (1/1000), anti-P-Src418 (1/1000), anti-FAK kinase (1/1000), anti-Y925-phospho FAK (1/1000), anti-Y397-phospho FAK and anti-Y861-phospho FAK (1/2000). Corresponding horseradish peroxidase-conjugated secondary Abs were used at 1/60 000 dilution. Immunoreactivity was visualized using the ECL+ system (Amersham).

Indirect immunofluorescence and correlation analysis. SrcY530F or SrcI-expressing cells, plated at low density on Matrigel for 2 d, were rinsed with PBS and fixed with 4% paraformaldehyde at room temperature for 15 min. After washes with PBS, cells were permeabilized with 0.2% Triton X-100 for 5 min and incubated 30 min with PBS/3% BSA. Cells were washed three times with PBS and incubated with primary Abs (all Abs diluted at 1/200 except for anti-cortactin diluted at 1/300) in PBS/0.2% BSA for 1 h at room temperature. After three additional washes, cells were incubated with Rhodamine Red X-conjugated secondary Abs in PBS/0.2% BSA (1/200 and 1/400 dilutions), washed with PBS and then observed using a confocal microscope (Bio-Rad 1024, Kr-Ar laser; Nikon Eclipse TE300, 60x water-immersion CFI Plan-Fluor objective, n. a. 1.2). GFP and rhodamine/FluoProbe 547 were excited at 488 and 568 nm respectively and fluorescence was collected at 522 (green) and 585 nm (red) respectively. For actin labelling, after paraformaldehyde and Triton treatments, cells were incubated with phalloidin fluoProbe 547 for 1 h at room temperature followed by three washes with PBS. For analysis of fluorescence intensities of SrcI-transfected cells, ImageJ software was used. Intensities at FAs in the green and red channels were plotted against each other and analyzed by linear regression using Prism software.

Live cell imaging. Cells expressing SrcI were plated at low density on Matrigel for 2 d and then treated or not with 100 μM pervanadate in EMEM supplemented with 10% FBS and 10 mM HEPES, prior to imaging by confocal microscopy as above (488 nm excitation, 522 nm emission). Z-series stacks (0.35 μm steps) were acquired every 5–10 min for 1 h at 32°C. Representative cells are illustrated from a minimum of four independent experiments. ImageJ software was used to assess the dynamics of FAs and membrane ruffles. FA disassembly was visualized and quantified as the loss of fluorescence in a selected region of interest (ROI) whereas membrane ruffle formation was quantified as a gain of fluorescence in a selected ROI. Since semi-logarithmic plots of the increase or decrease in fluorescence intensity at ruffles or focal adhesion respectively as a function of time were linear, rate constants were determined from the slope. Kymographs were constructed using ImageJ and the plugin from J. Rietdorf and A. Seitz.

FLIP (fluorescence loss in photobleaching). FLIP was used to determine whether SrcI distributes dynamically between two different compartments (FAs and membrane ruffles). SrcI-transfected cells were plated at low density on Matrigel for 2 d in EMEM supplemented with 10% FBS and 10 mM HEPES, prior to imaging by confocal microscopy as above (488 nm excitation, 522 nm emission) at 32 °C. A ROI to be bleached was specified for one compartment (e.g. FA) and an image was taken of the whole cell before bleaching, followed by bleaching of the ROI with full laser power at 488 nm for about 20 s and capture of another image at low laser power using a confocal microscope as above. This sequence was repeated four times. A loss in adjacent membrane ruffle fluorescence upon bleaching of FA indicates export of fluorescent proteins from the FA and shuttling between ruffles and the FA.

Results

Constitutively activated Src induces FAK phosphorylation and adhesion remodelling. We recently demonstrated that mutation of FAK at Tyr-397 results in impaired FA disassembly [30]. Upon autophosphorylation on Tyr-397 of FAK, Src kinase is the major tyrosine kinase recruited by FAK at FAs. Src is

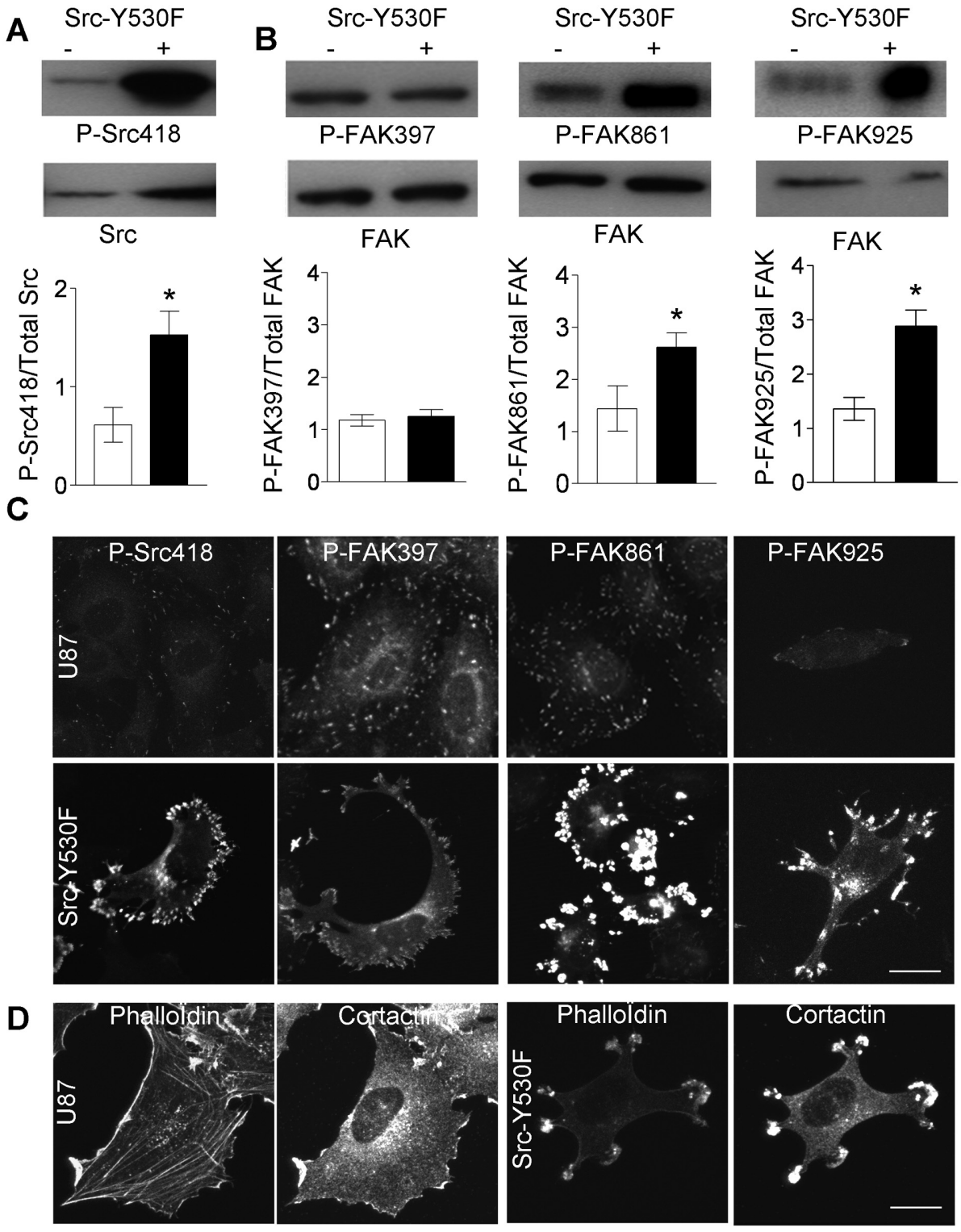

Figure 1. Effects of transfection of constitutively activated Src-Y530F in human U87 astrocytoma cells. Western blots of total cell lysates from control and Src-Y530F transfected cells probed with anti-PY418-Src Ab (*A*) and anti-phospho-specific FAK Abs against Tyr-397, Tyr-861 and Tyr-925 (*B*). Total amounts of proteins were monitored by stripping and reblotting with anti-Src or anti-FAK Abs. Histograms depict the ratio of densities of P-src over total Src or P-FAK over total FAK. Data are the mean ± s.e.m. (*$P<0.05$, paired *t*-test, relative to control) from at least three independent experiments. (*C*) Control (upper panels) and Src-Y530F transfected cells (lower panels) were fixed and stained with anti-P-Src Ab (leftmost panel), anti-P-FAK397 (left panel), anti-P-FAK861 (right panel) and anti-P-FAK925 (rightmost panel) Abs. Note the increase in phosphorylation of Src at Tyr-418 and FAK at Tyr-861 and Tyr-925, but not Tyr-397 in Src-Y530F-transfected cells. In transfected cells, note also the global change in cell shape with extensive membranes protrusions and the presence of podosomes at the periphery. (*D*) Control U87 cells and Src-Y530F cells were fixed and stained with phalloidin FluoProbe 547 (left) and anti-cortactin Ab (right).

believed to mediate FA disassembly via FAK phosphorylation processes as demonstrated using FAK with a mutated Src binding site [7], FAK with mutated Src-specific phosphorylation sites [1, 6, 18] and kinase dead mutants of Src [7]. Accordingly, activated Src should be able to induce FAK phosphorylation and FA disassembly. To verify this assumption, we transfected human U87 astrocytoma cells with a Src mutant in which Tyr-530 was substituted by phenylalanine (Src-Y530F). This point mutation is well known to lead to constitutively activated Src [31]. Indeed, as expected, U87-Src-Y530F cells displayed an increase in Src phosphorylation at Tyr-418, a hallmark of Src activation states [32] (Fig. 1A). Moreover, in Src-Y530F cells, enhanced phosphorylation of FAK at Tyr-861 and Tyr-925 was also observed (Fig. 1B). Both tyrosine sites are described as Src substrates [15, 33, 34], and phosphorylation of FAK at Tyr-925 has been implicated in FA disassembly [1, 18, 35, 36]. In contrast, Src-Y530F cells did not exhibit any change in FAK phosphorylation at Tyr-397 (Fig. 1B). To visualize the effect of Src-Y530F expression on the phosphorylation state of Src/FAK complexes at FAs, control U87 and Src-Y530F cells were fixed and stained with Abs against P-Y418-Src, P-Y397-FAK, P-Y861-FAK and P-Y925-FAK. In control cells, P-Y418-Src, P-Y397-FAK, P-Y861-FAK and P-Y925-FAK stainings were localized at FAs (Fig. 1C top). Upon Src-Y530F transfection, enhanced stainings for P-Y418-Src, P-Y861-FAK and P-Y925-FAK Abs but not with P-Y397-FAK Ab was observed at peripheral adhesion sites. This pattern was consistent with the phosphorylation state observed by Western blotting (Fig. 1C bottom). Furthermore, cell shape was noticeably changed in SrcY530F cells as compared to untransfected U87 cells, as SrcY530F cells did not display classical FAs but unusual peripheral adhesion sites with podosome rings that contain both cortactin and F-actin (Fig. 1D). This indicates that Src/FAK phosphorylation led to changes in peripheral cell-matrix attachment sites.

Use of Src Indicator as reporter of Src activation. In view of the local changes in both tyrosine phosphorylation and actin rearrangement observed upon Src activation, we characterized the dynamics of Src activation in living cells and its consequences on peripheral adhesion remodelling. To do so, we used Src Indicator (SrcI), a recently described fluorescence resonance energy transfer (FRET)-based Src reporter [37]. SrcI consists of fusions of CFP, the P-Y-binding domain of Src (SH2), a consensus substrate for Src (EIYGEF) and YFP (Fig. 2A). In NIH 3T3 and HeLa cells, stimulation of Src kinase activity by addition of PGDF or EGF causes 25–30 % changes in YFP to CFP emission ratio because of phosphorylation-induced changes in FRET [37]. However, in our study, activation of Src could not be detected by a FRET response (not shown) raising doubt on how FRET occurs as already reported [38]. Nevertheless, another P-tyrosine reporter was recently used to analyze the dynamics of proteins containing P-tyrosine in living cells, based on reporter intensity being linearly correlated with the labelling of an anti-P-tyrosine Ab [39]. For this reason, we chose to use SrcI as a reporter of Src activation without using the FRET function. To do so, the cellular distribution of SrcI was analyzed and the relative intensities of the reporter were compared to those of activated Src, assessed using an Ab that recognizes Src phosphorylation at Tyr-418.

After transfection in U87 cells, SrcI was localized at FAs as visualized with the YFP moiety of the construct, consistent with Src activation occurring mainly at these sites (Fig. 2B, left). It is well known that the localization of Src to FAs is actin-dependent [22, 29]. To verify that SrcI follows the dynamics of Src, cells were treated with cytochalasin D, an actin-disrupting drug. After treatment, SrcI was no longer localized at FAs (Fig. 2B, right), indicating that Src and SrcI have comparable cellular dynamics. In order to verify that Src activation was detected by SrcI, U87 cells were treated with pervanadate, a phosphatase inhibitor. Indeed, treatment with phosphatase inhibitors is known to increase both Src and FAK phosphorylation [1, 40–42], but also to induce peripheral adhesion rearrangement [1, 43, 44]. In our cells, addition of pervanadate induces Src activation as visualized in Western blots by the increase in P-SrcY418 levels both in non transfected and in SrcI-transfected U87 cells compared to non treated cells (Fig. 2C). The cellular distribution of SrcI and endogenous Src was also compared before and after pervanadate treatment. U87 cells stably transfected with SrcI were then fixed and stained with anti-P-Y418-Src Ab. We observed that SrcI (Fig. 2D, left panel green) co-localized with activated Src at FAs in (Fig. 2D, middle panel, red) before pervanadate treatment. After pervanadate, while a global increase in P-SrcY418 intensities could be detected, SrcI labelling was especially high at peripheral membranes where it co-localized with activated Src (Fig. 2D, lower panel). The relationship between P-Src Ab staining and SrcI labelling was further studied by plotting against each other the intensities of the two labels measured at individual FAs. The intensities of the two labels were linearly correlated in cells expressing SrcI (Fig. 3A), with the coefficient of correlation (r^2) ranging from 0.84 to 0.91. This indicates a high degree of correlation between the

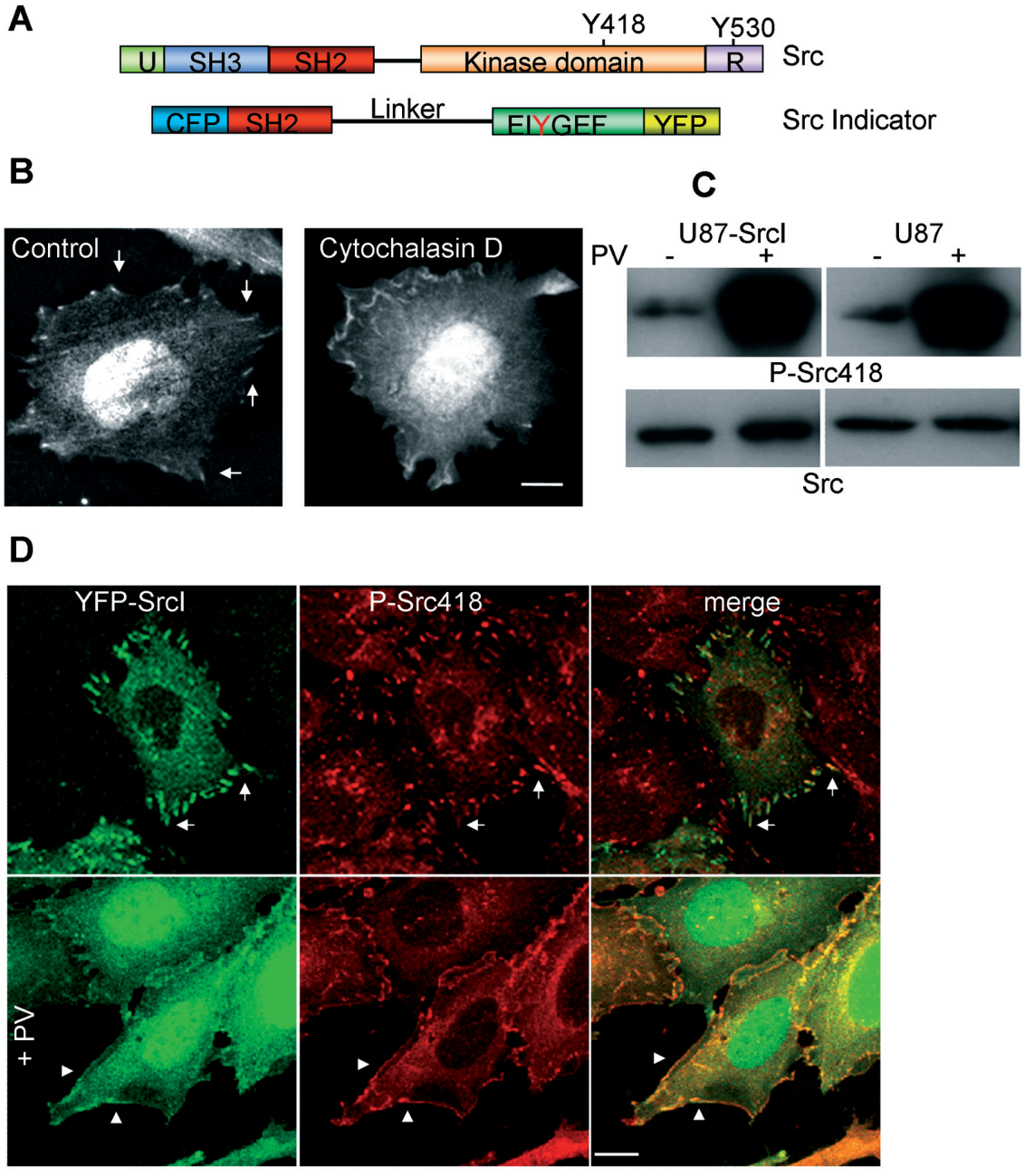

Figure 2. Subcellular localization and behaviour of Src Indicator. (*A*) The SrcI construction consists of fusions of CFP (blue), PY-binding domain of Src (SH2) (red), a consensus substrate for Src (green), and YFP (yellow). (*B*) In SrcI-transfected cells, SrcI localized at FAs (left). After cytochalasin D (10 μM) and disruption of the actin cytoskeleton, SrcI was no longer localized at FAs (right). Bar, 10 μm. (*C*) Western blots of total cell lysates from non transfected and SrcI-transfected U87 cells probed with anti-P-Src Ab show significant increases in Src phosphorylation upon pervanadate (PV) treatment. (*D*) Immunostaining with anti-P-Src Ab shows co-localization of SrcI (green) and activated Src (red) at FAs (arrows, upper panels). After 100 μM PV, note the disappearance of FAs and the co-localization of SrcI with P-Src at membrane ruffles (arrowheads, lower panels).

two labels. To exclude that SrcI is a broad spectrum marker of FA proteins, correlation analyses were performed with an anti-vinculin Ab in cells transfected with SrcI. While both proteins co-localized at FAs, (Fig. 3B), their respective intensities at FAs were essentially uncorrelated ($r^2 = 0.35$, Fig. 3B, right). These results further support that SrcI can be used as a marker of Src activation.

Dynamics of Src following pervanadate treatment. Based on the above analysis, we further examined the dynamics of Src activation in living cells transfected

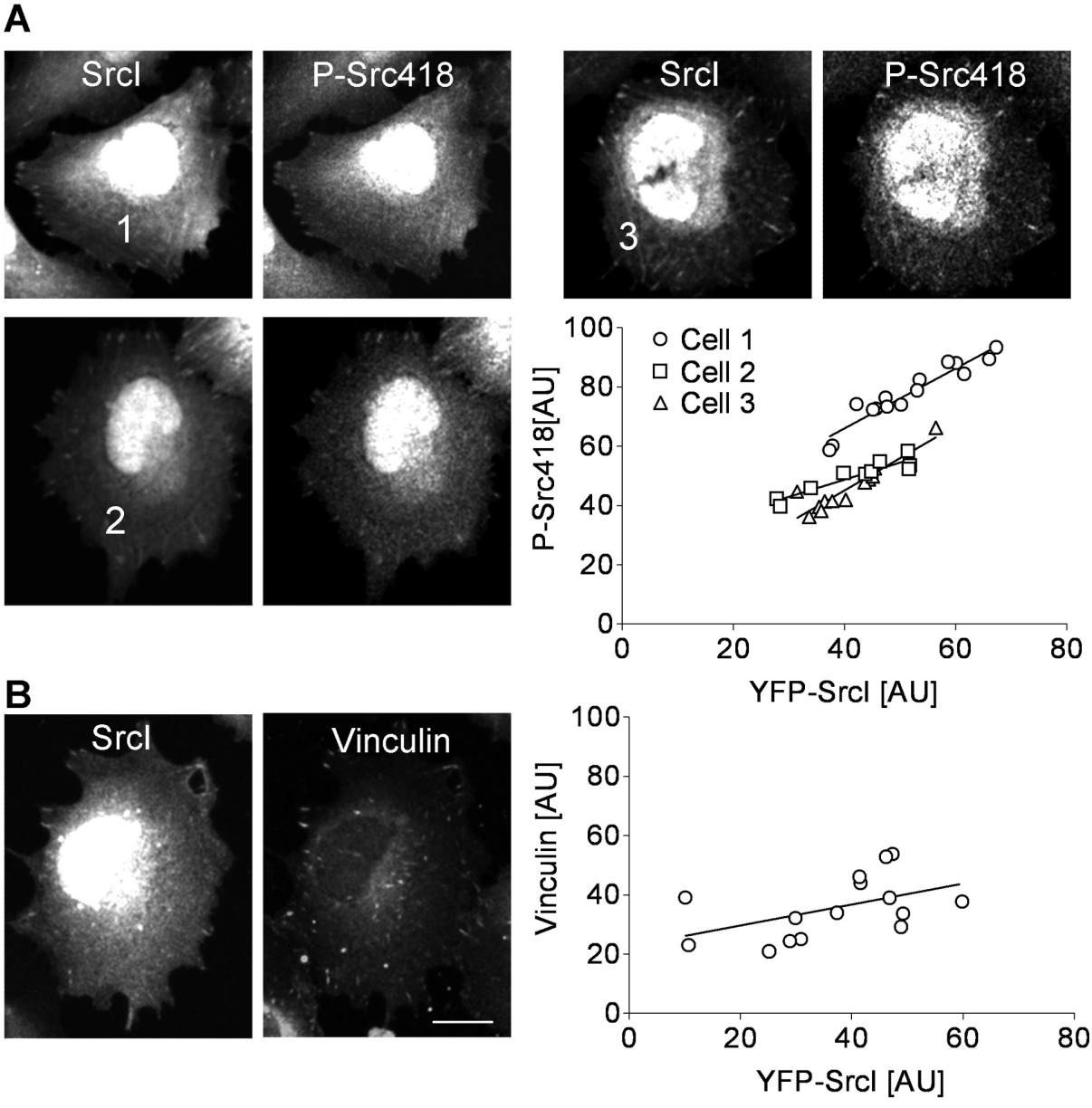

Figure 3. Use of SrcI as reporter of Src activation in live cells. (*A*) SrcI-transfected cells were fixed and labelled with anti-P-Src Ab. Note the co-localization of SrcI (left) and P-Src (right) at FAs (A, left and upper right). Correlation analysis of intensities of SrcI and P-Src (arbitrary units, AU) at individual FAs from SrcI-transfected cells confirms the linear relationship between SrcI and P-Src labelling (A, bottom right). (*B*) Fixed SrcI-transfected cells labelled with anti-vinculin Ab. Correlation between SrcI (left) and vinculin staining (right) at individual FAs was weak. Bar, 20 μm.

with SrcI and its consequence on peripheral adhesion rearrangement. Again, pervanadate treatment was used to activate Src, because of its well described effects on FA remodelling, which suggest a link between the kinase function of Src and actin rearrangement [1, 20]. Indeed, it has been shown that pervanadate-mediated FAK phosphorylation results in FAK departure from FAs, an effect linked to the activation of Src family kinases [1]. Within 20 min after pervanadate, fluorescence started to decrease at FAs, leading to an almost complete loss after 40–50 min of treatment (Fig. 4A). During this time, fluorescence appeared to localize at membrane ruffles (Fig. 4A, 40–50 min). To determine whether the decrease of fluorescence at FAs was time-correlated with the appearance of fluorescence at membrane ruffles, images from the time-lapse sequence were treated such that each resulting image was the subtraction of images at two time points separated by 10 min (Fig. 4B). Subtracted images were pseudo

colour-coded so that structures that remained unchanged between the two time points appeared in yellow, whereas new structures were red and those that disappeared were green. These data show that adhesion sites disappeared following addition of pervanadate and that *de novo* membrane ruffles were formed. It is noteworthy that the disappearance of fluorescence at FAs coincides with the appearance of fluorescence at ruffles both in the time-subtracted images (Fig. 4B) and in the kinetic analyses (Fig. 4A). This strongly suggests that upon phosphorylation, Src is translocated from FAs to membrane ruffles.

FA disassembly and membrane ruffle formation were quantified by determining their rates of disassembly and formation by integrating SrcI fluorescence intensities in individual FAs and membrane ruffles over time (Fig. 4C). The apparent rate constant for SrcI incorporation into ruffles was $3.55 \pm 0.23 \times 10^{-2}$ min^{-1}, and was similar to that off FA disassembly ($3.41 \pm 0.13 \times 10^{-2}$ min^{-1}). Since departure of Src from disassembling FAs and Src accumulation at membrane ruffles occur at the same rate, this strongly indicates that upon phosphorylation, Src is translocated from FAs to membrane ruffles.

Direct translocation of Src from focal adhesions to membrane ruffles. To confirm that Src is translocated from FAs to membrane ruffles upon activation, a confocal microscopy based method called Fluorescence Loss In Photobleaching (FLIP) was used. In this method, a cell compartment (in our case, containing a FA) is repetitively bleached and the global cellular fluorescence monitored between bleaching cycles (Fig. 5). A rapid loss in fluorescence in an adjacent non-bleached compartment (e.g. membrane ruffles) indicates that dynamic shuttling of fluorescent molecules occurs between the bleached and the non-bleached regions. In presence of pervanadate, FLIP experiments revealed that bleaching of fluorophores in an FA resulted in a 35 % decrease in fluorescence in adjacent membrane ruffles over a 20 s bleaching period compared to basal fluorescence, while distant cytosolic fluorescence was unchanged compared to basal fluorescence (Fig. 5B, C right panel).

Conventional video-microscopy did not allow determination of the dynamics of Src in the absence of pervanadate treatment, since membrane ruffle formation was essentially undetected (compare Fig. 5A and 5B left). In contrast, the high sensitivity of FLIP allowed to observe a 35 % decrease in adjacent membrane ruffle fluorescence following FA bleaching, while cytosolic fluorescence decreased only by 15 % (Fig. 5A, C left panel). These decreases are consistent with a rapid and dynamic equilibrium of activated Src between FAs and membrane ruffles. In cells co-transfected with SrcI and mRFP, analysis of FLIP experiments revealed that loss in mRFP fluorescence was equivalent in the membrane adjacent to the photobleached FA and in the cytosol, indicating that the active shuttling between FAs and ruffles was specific to SrcI (Fig. 5D).

Src inhibition prevents pervanadate-induced FA disassembly and membrane ruffle formation. To further evaluate the effect of pervanadate-induced Src phosphorylation in adhesion rearrangement, live cell imaging was carried out using SrcI-transfected cells pre-treated with PP2 (selective inhibitor of Src) or with PP3 (an inactive analogue of PP2). As described above, in control cells, several FAs disassembled after pervanadate, concomitant with formation of membrane ruffles. Upon pervanadate addition, the disassembly of FAs was confirmed using cells transfected with a GFP-FAK construct and the formation of ruffles was also confirmed using phase-contrast microscopy (not shown). Pervanadate-induced FA disassembly and ruffle formation were unchanged in PP3 pre-treated cells, whereas pre-treatment of cells with PP2 prevented both FA disassembly and formation of new membrane during the 1 h observation period (Fig. 6B). Quantification of FA disassembly in control cells revealed an apparent rate constant of $3.65 \pm 0.12 \times 10^{-2}$ min^{-1} which was significantly decreased to $0.22 \pm 0.08 \times 10^{-2}$ min^{-1} in the presence of PP2 but not PP3 (apparent rate constant of $2.82 \pm 0.16 \times 10^{-2}$ min^{-1}). Taken together, these results indicate that the activity of Src is needed to induce FA disassembly and formation of membrane ruffles following phosphorylation induced with pervanadate.

Src translocation from focal adhesions to membrane ruffles contributes to the formation of new adhesion sites. More detailed analysis of time-lapse movies revealed that membrane ruffles of pervanadate-treated SrcI-transfected cells displayed periodic extensions and retractions. The periodicity of this phenomenon was best seen in kymographs of the protruding cell edge (Fig. 7A, B), and is consistent with periodic waves of Src occurring during ruffle formation. Increased staining of activated Src was observed at the retracting cell edge and especially at the junction of retraction/extension interphase as visualized by line-profile analysis of kymographs (Fig. 7B, bottom). This suggests, firstly, that during the retraction period when the stiffness of the substratum is probed [45], Src is necessary and, secondly, that for the cell edge to stop retraction, P-Src accumulation at newly formed structures is also needed.

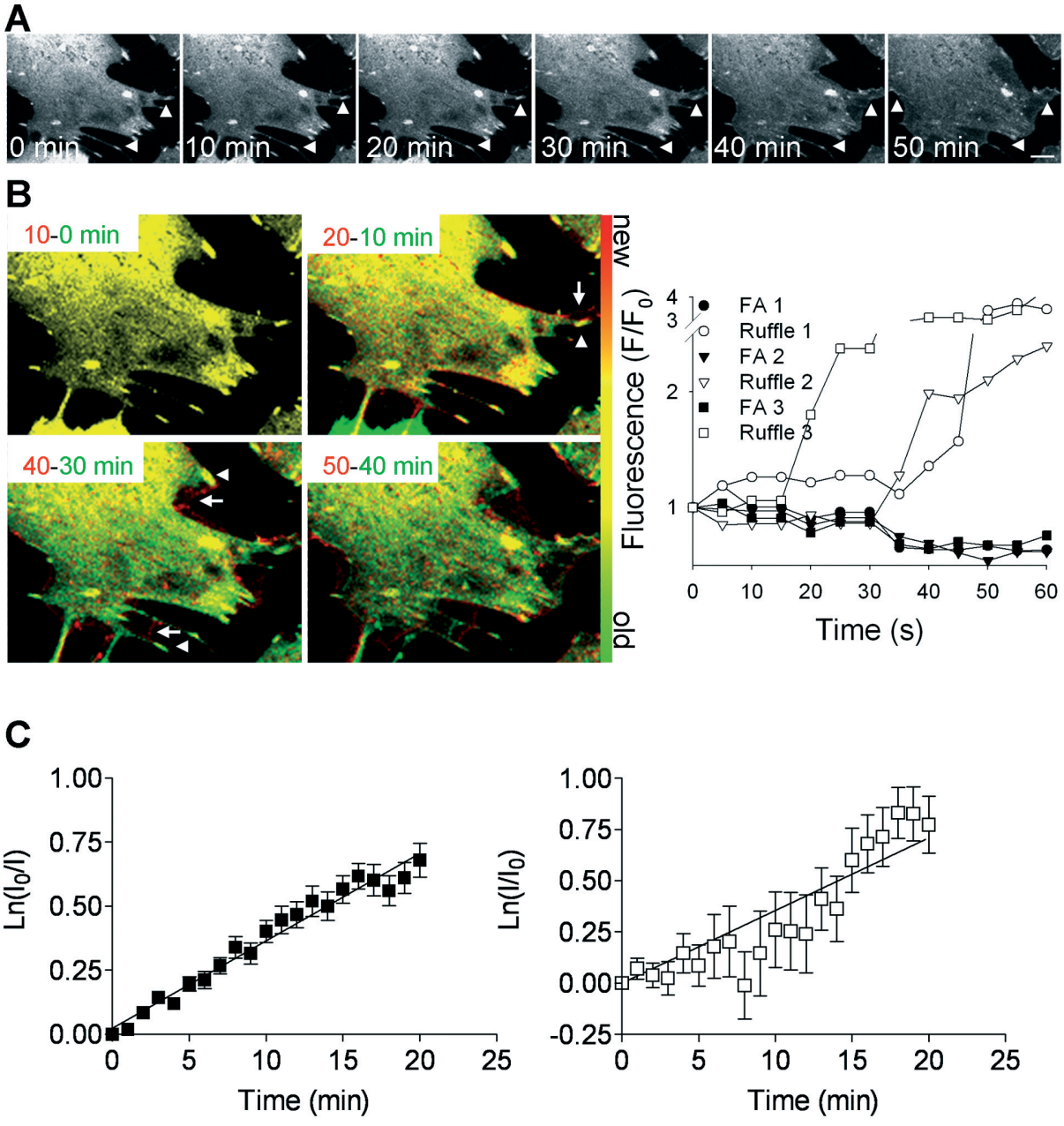

Figure 4. Dynamics of Src following pervanadate. (*A*) Time-lapse confocal microscopy of SrcI-transfected cells after PV treatment during 50 min (see Video 1). Note the time-correlated dissociation of FAs and formation of membrane ruffles (arrowheads). (*B*) Images from A were analyzed by temporal subtraction imaging (intensity values of each image were subtracted by the intensity values in the image taken 10 min earlier). Appearance of new structures is depicted in red, while structures that had disappeared are green, and yellow denotes unchanged structures. Bars, 5 μm. Graph represents fluorescence intensities normalized to fluorescence intensity at t = 0 over a 60 min time period. Representative measurements done at membrane ruffles (full shapes corresponding to arrows) and at FAs (empty shapes corresponding to arrowheads) were plotted. (*C*) Time courses of FA disassembly (left) and membrane ruffle formation (right). Data are mean ± s.e.m. (n = 21 FAs and membrane ruffles) of the ratio of the integrated fluorescence intensity at each time point relative to initial intensity. Rate constants of FA disassembly and membrane ruffle formation were calculated from the slopes of the lines.

Discussion

In the present study, we demonstrate that Src activation induces changes in astrocytoma cell morphology involving formation of podosome enriched in phosphorylated FAK protein. Kinetic analyses of Src activation reveal high Src trafficking from FAs to membrane ruffles during actin rearrangement and highlight the role of Src activity in adhesion remodelling.

It is well known that cell transformation by oncogenic Src causes disruption of actin stress fibers, disintegra-

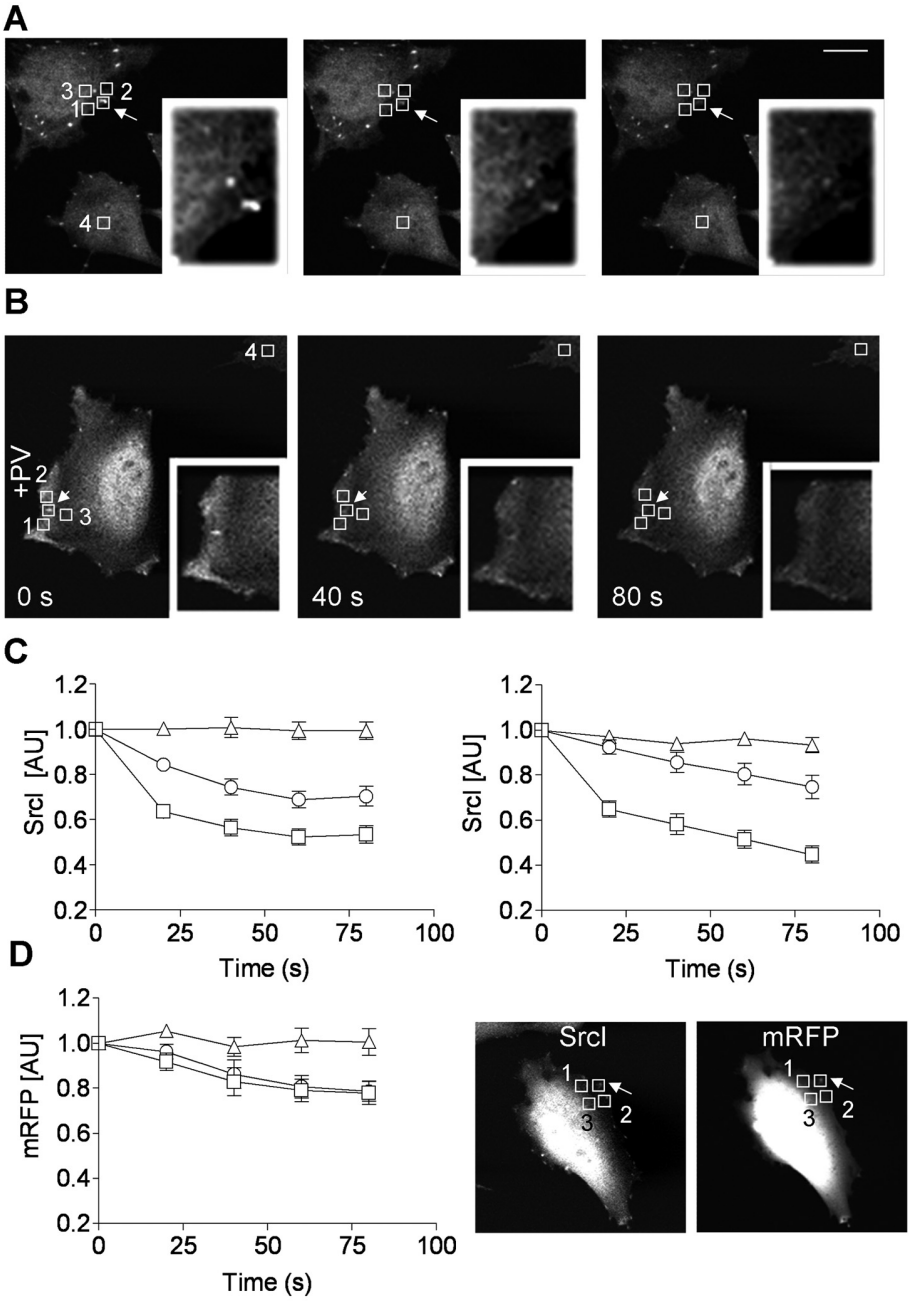

Figure 5. Src trafficking between FAs and membrane ruffles. FLIP experiments on SrcI-transfected-cells in absence (*A*) or presence of PV (*B*) reveal Src dynamics after departure from FAs. The region of interest including an FA (white square indicated by the arrow) was repetitively bleached (four times) with maximum laser power for 20 s. After each photobleach cycle, an image of the entire field was acquired at normal laser intensity. Fluorescence intensities were measured in individual ROIs (white squares) at membranes adjacent to the photobleached FAs (squares 1 and 2), in the cytosol of the photobleached cell (square 3), and in neighbouring cells (square 4). Note the loss in fluorescence in membranes adjacent to the photobleached FA (insets) (*C*) Graphs represent normalized fluorescence intensities to the initial intensities in different compartments indicated in A over time (triangle: neighbour cell, circle: cytoplasm, square: ruffles). Note the rapid loss of 35 % of the initial intensity at membrane ruffles in PV-treated cells (right panel). In control cells, whereas the same loss of initial intensity at membrane ruffles was observed, this was accompanied by about 15 % of loss of intensity in the cytosol of photobleached cells (left panel). Mean ± s.e.m. of 16 measurements from four separate experiments. Bar, 20 μm. (*D*) U87 cotransfected with Src I and mRFP plasmids were submitted to FLIP experiments under conditions identical to those described hereinbefore. Graph represents normalized mRFP fluorescence intensities to initial intensities in compartments adjacent to the photobleached area indicated by an arrow (triangle: neighbour cell, circle: cytoplasm, square: ruffles). Note the same loss in mRFP fluorescence intensities in membrane ruffles and cytosol over time.

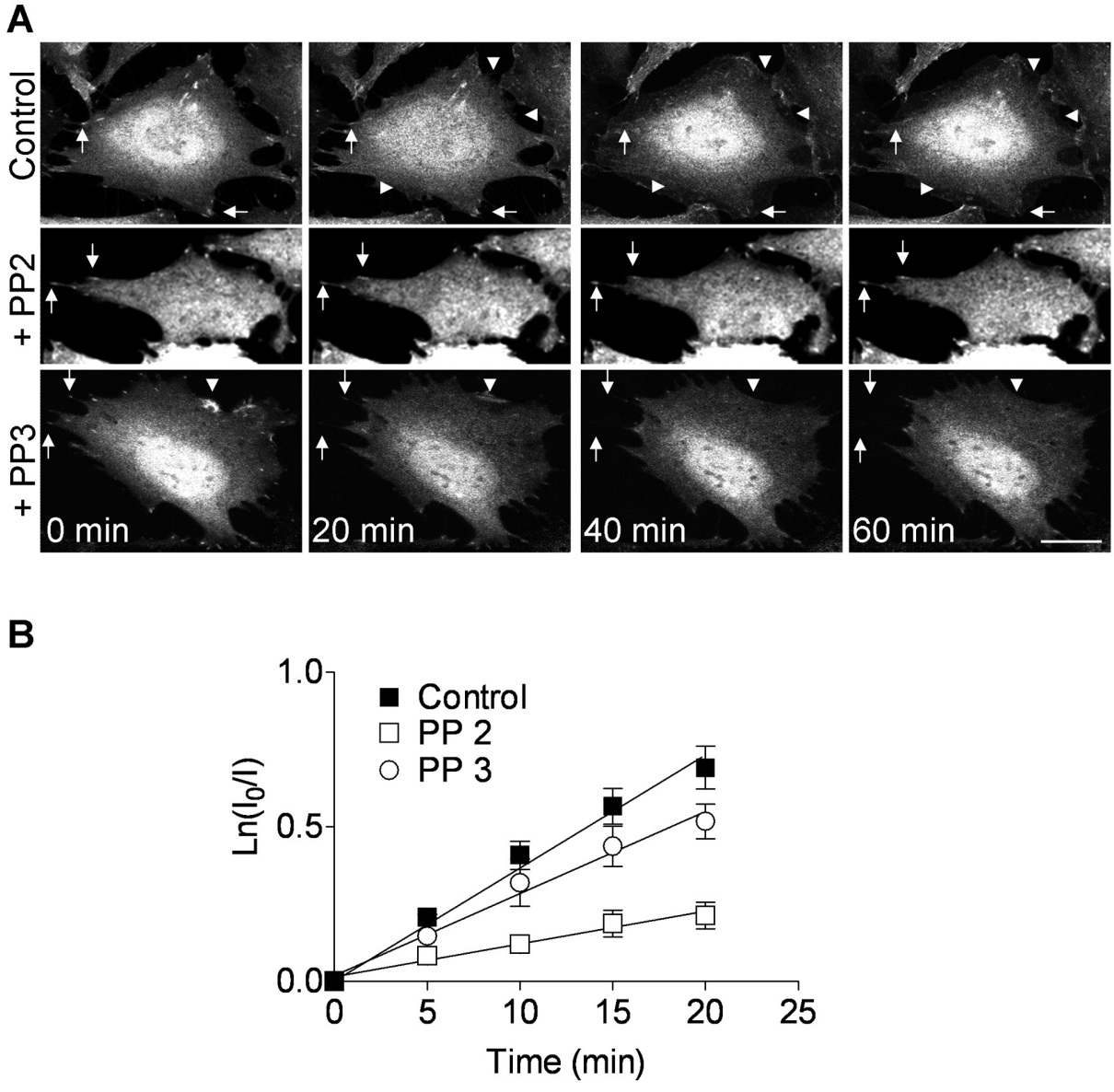

Figure 6. Src activity is necessary for Src translocation from FAs to membrane ruffles. (*A*) Time-lapse microscopy of SrcI-expressing cells during 60 min after PV addition in the absence of (top panels; see also Video 2) and after pre-treatment with PP2 (10 μM, 30 min; middle panels; see also Video 3) or with PP3 (10 μM, 30 min; lower panels; see also Video 4). In the absence of PP2, or in the presence of PP3, SrcI-labelled FAs disappeared (arrows) concomitant with the appearance of fluorescence at membrane ruffles (arrowheads), unlike in PP2-pretreated cells. (*C*) The graph represents the quantification of fluorescence intensities at FAs. Data are mean ± s.e.m. of the ratio of the integrated fluorescence intensity of FAs at each time point relative to initial intensity from 3–4 independent experiments. Note the constant rate of decrease of fluorescence at FAs in control cells (closed squares) or PP3-pretreated cells (open circles) which is highly reduced in PP2-pretreated cells (open squares). Bar, 20 μm.

tion of adhesion plaques and formation of invasive adhesions called podosomes [46, 47]. However, the exact implication of Src in mediating these processes is not well understood. Dissociation of FAs implicates Src-mediated FAK phosphorylation [6, 7] and, in particular, phosphorylation at FAK Tyr-925 is required for efficient FA turn-over [16]. In cells transfected with Src-Y530F, a constitutively activated form of Src, we observed increased FAK Tyr-925 phosphorylation in podosome. This suggests that activated Src is required for efficient remodelling of FAs into podosomes (Fig. 1), in agreement with previous studies [20] using cells transfected with Src-Y527F (the chicken counterpart of human Src-Y530F). Indeed, Src-Y527F cells – although well spread – had little or no actin stress fiber formation, were not polarized, had aberrant FA formation and cell shape and high levels of FAK phosphorylation [20]. Importantly, using a

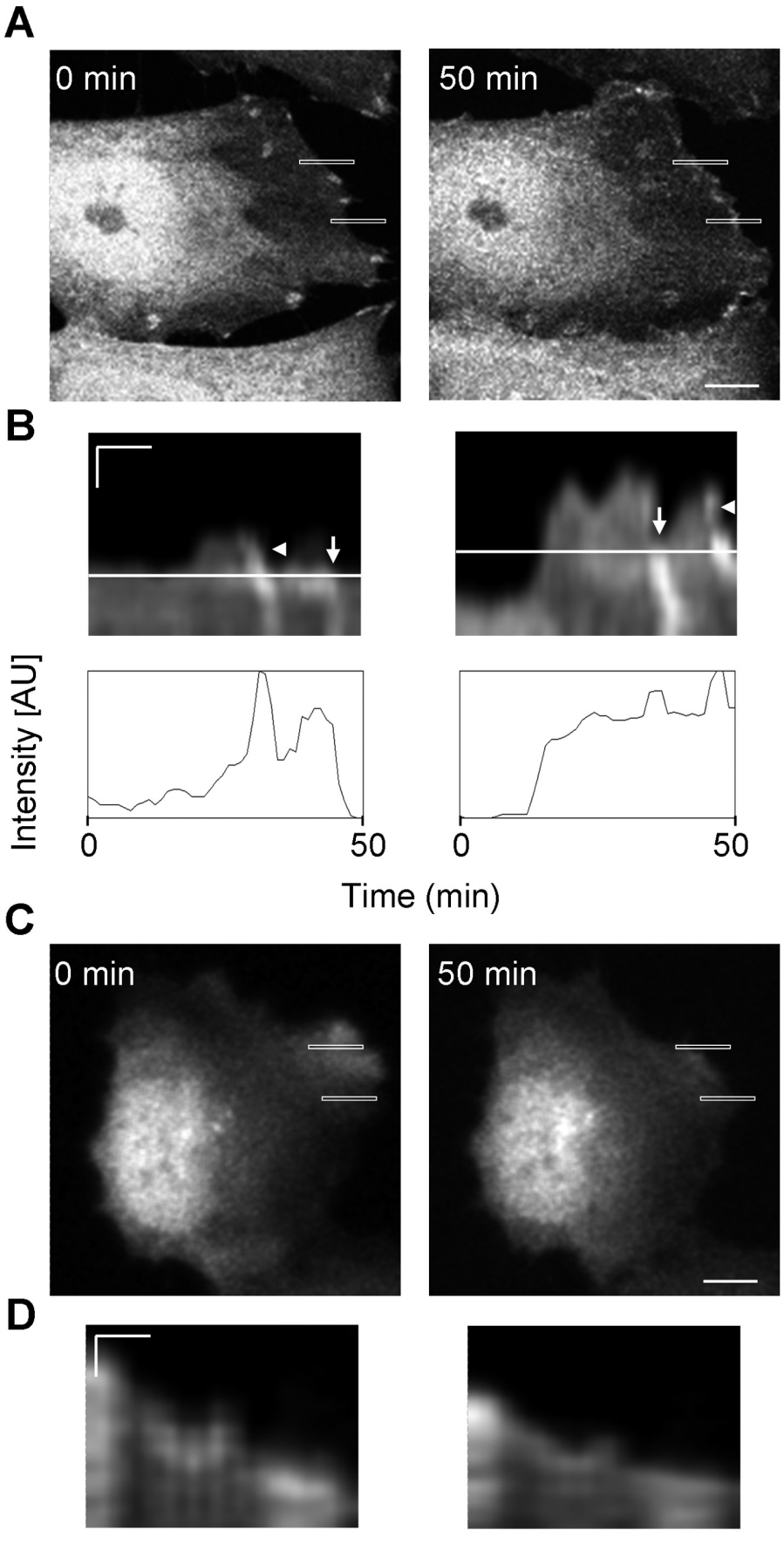

Figure 7. Pervanadate induces cycling of membrane extension/retraction. (*A*) Confocal microscopy images of SrcI-transfected cells before (left) and after PV treatment (45 min, 100 μM, right). Note membrane extension/retraction at the leading edge together with dissociation of FAs (see also Video 5). (*B*) Kymographs of a SrcI-transfected cell (upper panels). The rectangles in (*A*) depict the regions used to generate the kymographs (beginning of the kymograph on the left and the end on the right), with the upper rectangle corresponding to the left kymograph and lower rectangle to the right kymograph. Scale bars: 10 min (x-direction), 1 μm (y-direction). This representation allows clear visualisation of the extension/retraction cycle of the membrane during PV treatment. The lower panels correspond to SrcI intensities along the lines depicted in white in the kymographs. Note high intensities during the retraction period (arrowheads) and at the junction of the retraction/extension cycle (arrows). (*C*) Confocal microscopy images of mRFP-transfected cells before (left) and after PV treatment (45 min, 100 μM, right). Note membrane extension/retraction at the leading edge. (*D*) Kymographs of mRFP-transfected cell. Note that, in contrast to that observed with SrcI, no accumulation of mRFP was detected at the junction of the retraction/extension cycle.

mutated form of Src with a non functional SH2 phospho-tyrosine binding site (R175L-SH2), it was shown that Src/FAK interaction is necessary for efficient targeting of Src to FAs. Nevertheless, incorporating the FAT (FA Targeting) domain of FAK into the Src R175L-SH2 mutant, while targeting the latter construct to FAs, did not restore morphological transformation observed with activated Src [20]. This suggests that Src location at FAs may not be the sole determinant of adhesion remodelling and highlight the role of Src SH2 domain.

However, using the viral oncoprotein v-Src, it was shown that FAK phosphorylation and FA loss during transformation require the kinase activity of Src [48]. Src kinase activity is also necessary for the efficient remodelling of cellular adhesion [29]. Indeed, using Src251, a truncated form of Src that lacks the kinase domain, it was demonstrated that upon PDGF stimulation, although Src251 was still able to traffic out of FAs, lamellipodia formation was impaired [29]. Taken together, these studies imply that Src trafficking is a fundamental aspect of Src-mediated cell transformation, resulting in Src localization in subcellular structures where both its SH2 domain and its kinase activity are needed for actin rearrangement. Using a combination of kinetic analysis and FLIP techniques, we have shown that upon activation, Src is translocated from FAs to membrane ruffles (Fig. 4, 5), where Src activity is needed for adhesion remodelling. Indeed, pharmacological inhibition of Src inhibits both FA disassembly and ruffle formation.

Direct translocation of Src to newly formed membrane may occur via different pathways, including actin-dependent mechanisms or lateral membrane diffusion. Recently, it has been shown that the lateral diffusion of constitutively active Src is three-fold slower than wild type Src, implying that lateral diffusion is slowed by interaction of activated Src with membrane and/or membrane-associated proteins [49]. This decrease in mobility required both an intact SH2 domain and Src kinase activity, suggesting that Src binds to membrane-associated proteins that Src had phosphorylated [49]. It is thus possible that activated Src traffics from FAs to adjacent membrane ruffles via lateral diffusion of multimolecular complexes and, in agreement, we observed colocalization of FAK with activated Src at membrane ruffles upon pervanadate treatment (not shown). Consistently, a transient accumulation of a signalling complex containing FAK, Src, p130Cas and Dock180 at lamellipodia has been described during cell invasion [24]. On the other hand, several studies have shown that Src trafficking is actin-dependent [22, 48, 50], indicating that actin formation would be a prerequisite for Src translocation from FAs to membrane ruffles. Upon Rac 1 activation, actin polymerization at the plasma membrane produces edge ruffles and lamellipodia [51, 52]. Our examination of the dynamics of ruffle formation shows that the initial event was the formation of membrane between two adjacent FAs (Fig. 4B). In accordance, using micropatterned extracellular matrix arrays, it was reported that during spreading, adhesion structures were first stabilized by contact with the adhesive plots and subsequently converted into lamellipodia-like extensions starting at the filopodia tips. An analysis of the physical mechanism of spreading revealed that, after filopodia projection and focal complex formation, actin then organizes to form cortical cytoskeletal bridges between filopodia, a process promoted by Src [53]. Therefore, an interesting possibility is that the translocation of Src from FAs to membrane ruffles occurs via cortical actin that bridges adjacent focal adhesions, a process dependent upon Src activation. This is supported by the similar rates of SrcI incorporation into membrane ruffles and of SrcI loss from FAs (Fig. 4C), and also by the PP2-induced inhibition of FA disassembly and ruffle formation (Fig. 6). Finally, it should be noted here that as reported recently, the signal of a FRET-based reporter at a given spot results from the local kinase activity acting on the reporter plus the signal of the activated reporter diffusing into the cell [54]. The diffusion of the reporter could therefore reduce the cumulative signal produced by the kinase activity. In our case, because SrcI lacks the membrane anchor of endogenous Src, its diffusion within the cell should be faster than that of Src. This difference could alter the rates of Src when exchanging between FAs and membrane ruffles, resulting in an underestimation of the rapid shuttling of Src between the two locations. Nevertheless, since in our study we did not use SrcI as a FRET-based reporter, our analyses are not biased by the two populations of reporters (one activated and one inactivated) with different fluorescence responses, thus limiting the effect of the rapid diffusion of SrcI on the estimation of the exchange rate of Src.

What might be the significance of rapid Src shuttling between FAs and membrane ruffles? Recently, local periodic contractions of lamellipodia have been shown to correlate with rearwards actin waves [45]. These actin waves bind a signalling complex which is transported locally from the tip to the base of the lamellipodium, activating the next contraction/extension cycle. This cycle is needed to probe the rigidity of the extracellular matrix so that the contraction event leads to the formation of nascent adhesion sites. Kymograph analysis of pervanadate-treated cells revealed high ruffling activities at the leading edge (Fig. 7). Of importance, SrcI intensity was especially

high during the retraction period and at the junction of the contraction/extension cycle, consistent with a role for activated Src in the formation of nascent adhesion sites and in agreement with a previous study showing that newly formed complexes are highly tyrosine phosphorylated [3]. Thus, we propose that Src phosphorylation couples FA disassembly to membrane ruffling, aimed at probing surface rigidity, and ultimately to FA formation when the retraction period stops. Rapid shuttling of Src between FAs and the plasma membrane would therefore allow a gain in reactivity to a given stimulus. This would promote enhanced migration by synchronizing FA disassembly and lamellipodial extension.

Electronic supplementary material. Supplementary material is available in the online version of this article at springerlink.com (DOI 10.1007/s00018-008-8424-4) and is accessible for authorized users.

Acknowledgements. We thank R. Y. Tsien (Dept. of Pharmacology, UCSD, CA 92093, USA) and F. Cruzalegui (Division of Cancer Research, Institut de Recherches Servier, France) for kindly providing plasmids. We thank F. Saltel (IECB, U889, France) and H. de Rocquigny (UMR7175, Faculté de Pharmacie, France) for kindly providing the cortactin antibody and the mRFP pcDNA3 plasmid, respectively. The work was supported by grants from the Ligue Nationale Contre le Cancer (Comité du Bas Rhin) to P. Rondé. A. Hamadi was supported by a fellowship from the Ministère de la Recherche. T. B. Deramaudt was supported by a fellowship from the CNRS.

1 Katz, B. Z., Romer, L., Miyamoto, S., Volberg, T., Matsumoto, K., Cukierman, E., Geiger, B. and Yamada, K. M. (2003). Targeting membrane-localized focal adhesion kinase to focal adhesions: roles of tyrosine phosphorylation and SRC family kinases. J. Biol. Chem. 278, 29115–29152.
2 Frame, M. C. (2002). Src in cancer: deregulation and consequences for cell behaviour. Biochim. Biophys. Acta 1602, 114–130.
3 Zaidel-Bar, R., Cohen, M., Addadi, L. and Geiger, B. (2004). Hierarchical assembly of cell-matrix adhesion complexes. Biochem. Soc. Trans. 32, 416–420.
4 Zaidel-Bar, R., Itzkovitz, S., Ma'ayan, A., Iyengar, R. and Geiger, B. (2007). Functional atlas of the integrin adhesome. Nat. Cell Biol. 9, 858–867.
5 Summy, J. M. and Gallick, G. E. (2003). Src family kinases in tumor progression and metastasis. Cancer Metastasis Rev 22, 337–358.
6 Westhoff, M..A., Serrels, B., Fincham, V. J., Frame, M. C. and Carragher, N. O. (2004). SRC-mediated phosphorylation of focal adhesion kinase couples actin and adhesion dynamics to survival signaling. Mol. Cell Biol. 24, 8113–8133.
7 Webb, D. J., Donais, K., Whitmore, L. A., Thomas, S. M., Turner, C. E., Parsons, J. T. and Horwitz, A. F. (2004). FAK-Src signalling through paxillin, ERK and MLCK regulates adhesion disassembly. Nat. Cell Biol. 6, 154–161.
8 Lipfert, L., Haimovich, B., Schaller, M. D., Cobb, B. S., Parsons, J. T. and Brugge, J. S. (1992). Integrin-dependent phosphorylation and activation of the protein tyrosine kinase pp125FAK in platelets. J. Cell Biol. 119, 905–912.
9 Schaller, M. D., Hildebrand, J. D., Shannon, J. D., Fox, J. W., Vines, R. R. and Parsons, J. T. (1994). Autophosphorylation of the focal adhesion kinase, pp125FAK, directs SH2-dependent binding of pp60src. Mol. Cell Biol. 14, 1680–1688.
10 Kornberg, L. J., Earp, H. S., Turner, C. E., Prockop, C. and Juliano, R. L. (1991). Signal transduction by integrins: increased protein tyrosine phosphorylation caused by clustering of beta 1 integrins. Proc. Natl. Acad. Sci. USA 88, 8392–8396.
11 Kornberg, L., Earp, H. S., Parsons, J. T., Schaller, M. and Juliano, R. L. (1992). Cell adhesion or integrin clustering increases phosphorylation of a focal adhesion-associated tyrosine kinase. J. Biol. Chem. 267, 23439–23494.
12 Calalb, M. B., Polte, T. R. and Hanks, S. K. (1995). Tyrosine phosphorylation of focal adhesion kinase at sites in the catalytic domain regulates kinase activity: a role for Src family kinases. Mol. Cell Biol. 15, 954–963.
13 Xing, Z., Chen, H. C., Nowlen, J. K., Taylor, S. J., Shalloway, D. and Guan, J. L. (1994). Direct interaction of v-Src with the focal adhesion kinase mediated by the Src SH2 domain. Mol. Biol. Cell 5, 413–421.
14 Owens, L. V., Xu, L., Craven, R. J., Dent, G. A., Weiner, T. M., Kornberg, L., Liu, E. T. and Cance, W. G. (1995). Overexpression of the focal adhesion kinase (p125FAK) in invasive human tumors. Cancer Res. 55, 2752–2755.
15 Calalb, M. B., Zhang, X., Polte, T. R. and Hanks, S. K. (1996). Focal adhesion kinase tyrosine-861 is a major site of phosphorylation by Src. Biochem. Biophys. Res. Commun. 228, 662–668.
16 Brunton, V. G., Avizienyte, E., Fincham, V. J., Serrels, B., Metcalf, C. A., 3rd, Sawyer, T. K. and Frame, M. C. (2005). Identification of Src-specific phosphorylation site on focal adhesion kinase: dissection of the role of Src SH2 and catalytic functions and their consequences for tumor cell behavior. Cancer Res. 65, 1335–1342.
17 Schlaepfer, D. D., Broome, M. A. and Hunter, T. (1997). Fibronectin-stimulated signaling from a focal adhesion kinase-c-Src complex: involvement of the Grb2, p130cas, and Nck adaptor proteins. Mol. Cell Biol. 17, 1702–1713.
18 Avizienyte, E., Brunton, V. G., Fincham, V. J. and Frame, M. C. (2005). The SRC-induced mesenchymal state in late-stage colon cancer cells. Cells Tissues Organs 179, 73–80.
19 Cary, L. A., Klinghoffer, R. A., Sachsenmaier, C. and Cooper, J. A. (2002). SRC catalytic but not scaffolding function is needed for integrin-regulated tyrosine phosphorylation, cell migration, and cell spreading. Mol. Cell Biol. 22, 2427–2440.
20 Yeo, M. G., Partridge, M. A., Ezratty, E. J., Shen, Q., Gundersen, G. G. and Marcantonio, E. E. (2006). Src SH2 arginine 175 is required for cell motility: specific focal adhesion kinase targeting and focal adhesion assembly function. Mol. Cell Biol. 26, 4399–4409.
21 Thomas, J. W., Ellis, B., Boerner, R. J., Knight, W. B., White, G. C., 2nd and Schaller, M.D. (1998). SH2- and SH3-mediated interactions between focal adhesion kinase and Src. J. Biol. Chem. 273, 577–583.
22 Fincham, V. J., Brunton, V. G. and Frame, M. C. (2000). The SH3 domain directs acto-myosin-dependent targeting of v-Src to focal adhesions via phosphatidylinositol 3-kinase. Mol. Cell Biol. 20, 6518–6536.
23 Hauck, C. R., Hsia, D. A., Ilic, D. and Schlaepfer, D. D. (2002). v-Src SH3-enhanced interaction with focal adhesion kinase at beta 1 integrin-containing invadopodia promotes cell invasion. J. Biol. Chem. 277, 12487–12479.
24 Hsia, D. A., Mitra, S. K., Hauck, C. R., Streblow, D. N., Nelson, J. A., Ilic, D., Huang, S., Li, E., Nemerow, G. R., Leng, J., Spencer, K. S., Cheresh, D. A. and Schlaepfer, D. D. (2003). Differential regulation of cell motility and invasion by FAK. J. Cell Biol. 160, 753–767.
25 Veracini, L., Franco, M., Boureux, A., Simon, V., Roche, S. and Benistant, C. (2006). Two distinct pools of Src family tyrosine kinases regulate PDGF-induced DNA synthesis and actin dorsal ruffles. J. Cell Sci. 119, 2921–2934.
26 Chang, J. H., Gill, S., Settleman, J. and Parsons, S. J. (1995). c-Src regulates the simultaneous rearrangement of actin cytoskeleton, p190RhoGAP, and p120RasGAP following epidermal growth factor stimulation. J. Cell Biol. 130, 355–368.

27 Moissoglu, K. and Gelman, I. H. (2003). v-Src rescues actin-based cytoskeletal architecture and cell motility and induces enhanced anchorage independence during oncogenic transformation of focal adhesion kinase-null fibroblasts. J/ Biol. Chem. 278, 47946–47965.
28 Felsenfeld, D. P., Schwartzberg, P. L., Venegas, A., Tse, R. and Sheetz, M. P. (1999). Selective regulation of integrin–cytoskeleton interactions by the tyrosine kinase Src. Nat. Cell Biol. 1, 200–206.
29 Timpson, P., Jones, G. E., Frame, M. C. and Brunton, V. G. (2001). Coordination of cell polarization and migration by the Rho family GTPases requires Src tyrosine kinase activity. Curr. Biol. 11, 1836–1846.
30 Hamadi, A., Bouali, M., Dontenwill, M., Stoeckel, H., Takeda, K. and Ronde, P. (2005). Regulation of focal adhesion dynamics and disassembly by phosphorylation of FAK at tyrosine 397. J. Cell Sci. 118, 4415–4425.
31 Reynolds, A. B., Vila, J., Lansing, T. J., Potts, W. M., Weber, M. J. and Parsons, J. T. (1987). Activation of the oncogenic potential of the avian cellular src protein by specific structural alteration of the carboxy terminus. Embo J. 6, 2359–2364.
32 Piwnica-Worms, H., Saunders, K. B., Roberts, T. M., Smith, A. E. and Cheng, S. H. (1987). Tyrosine phosphorylation regulates the biochemical and biological properties of pp60c-src. Cell 49, 75–82.
33 Abu-Ghazaleh, R., Kabir, J., Jia, H., Lobo, M. and Zachary, I. (2001). Src mediates stimulation by vascular endothelial growth factor of the phosphorylation of focal adhesion kinase at tyrosine 861, and migration and anti-apoptosis in endothelial cells. Biochem. J. 360, 255–264.
34 Schlaepfer, D. D. and Hunter, T. (1996). Evidence for in vivo phosphorylation of the Grb2 SH2-domain binding site on focal adhesion kinase by Src-family protein-tyrosine kinases. Mol. Cell Biol. 16, 5623–5633.
35 Dixon, R. D., Chen, Y., Ding, F., Khare, S. D., Prutzman, K. C., Schaller, M. D., Campbell, S. L. and Dokholyan, N. V. (2004). New insights into FAK signaling and localization based on detection of a FAT domain folding intermediate. Structure 12, 2161–2171.
36 Prutzman, K. C., Gao, G., King, M. L., Iyer, V. V., Mueller, G. A., Schaller, M. D. and Campbell, S. L. (2004). The focal adhesion targeting domain of focal adhesion kinase contains a hinge region that modulates tyrosine 926 phosphorylation. Structure 12, 881–891.
37 Ting, A. Y., Kain, K. H., Klemke, R. L. and Tsien, R. Y. (2001). Genetically encoded fluorescent reporters of protein tyrosine kinase activities in living cells. Proc. Natl. Acad. Sci. USA 98, 15003–15008.
38 Wang, Y., Botvinick, E. L., Zhao, Y., Berns, M. W., Usami, S., Tsien, R. Y. and Chien, S. (2005). Visualizing the mechanical activation of Src. Nature 434, 1040–1045.
39 Kirchner, J., Kam, Z., Tzur, G., Bershadsky, A. D. and Geiger, B. (2003). Live-cell monitoring of tyrosine phosphorylation in focal adhesions following microtubule disruption. J. Cell Sci. 116, 975–986.
40 Boulven, I., Robin, P., Desmyter, C., Harbon, S. and Leiber, D. (2002). Differential involvement of Src family kinases in pervanadate-mediated responses in rat myometrial cells. Cell Signal 14, 341–349.
41 Takahashi, H., Suzuki, K. and Namiki, H. (2004). Pervanadate-induced reverse translocation and tyrosine phosphorylation of phorbol ester-stimulated protein kinase C betaII are mediated by Src-family tyrosine kinases in porcine neutrophils. Biochem. Biophys. Res. Commun. 314, 830–837.
42 Feick, P., Gilhaus, S. and Schulz, I. (1998). Pervanadate stimulates amylase release and protein tyrosine phosphorylation of paxillin and p125(FAK) in differentiated AR4–2J pancreatic acinar cells. J. Biol. Chem. 273, 16366–16367.
43 Herrera Abreu, M. T., Wang, Q., Vachon, E., Suzuki, T., Chow, C. W., Wang, Y., Hong, O., Villar, J., McCulloch, C. A. and Downey, G. P. (2006). Tyrosine phosphatase SHP-2 regulates IL-1 signaling in fibroblasts through focal adhesions. J. Cell Physiol. 207, 132–143.
44 Crean, J. K., Furlong, F., Finlay, D., Mitchell, D., Murphy, M., Conway, B., Brady, H. R., Godson, C. and Martin, F. (2004). Connective tissue growth factor [CTGF]/CCN2 stimulates mesangial cell migration through integrated dissolution of focal adhesion complexes and activation of cell polarization. Faseb J. 18, 1541–1543.
45 Giannone, G., Dubin-Thaler, B. J., Dobereiner, H. G., Kieffer, N., Bresnick, A. R. and Sheetz, M. P. (2004). Periodic lamellipodial contractions correlate with rearward actin waves. Cell 116, 431–443.
46 Nakamura, N., Tanaka, J. and Sobue, K. (1993). Rous sarcoma virus-transformed cells develop peculiar adhesive structures along the cell periphery. J. Cell Sci. 106 (Pt 4), 1057–1069.
47 Brands, R., de Boer, A., Feltkamp, C. A. and Roos, E. (1990). Disintegration of adhesion plaques in chicken embryo fibroblasts upon Rous sarcoma virus-induced transformation: different dissociation rates for talin and vinculin. Exp. Cell Res. 186, 138–148.
48 Fincham, V. J. and Frame, M. C. (1998). The catalytic activity of Src is dispensable for translocation to focal adhesions but controls the turnover of these structures during cell motility. Embo J. 17, 81–92.
49 Shvartsman, D. E., Donaldson, J. C., Diaz, B., Gutman, O., Martin, G. S. and Henis, Y. I. (2007). Src kinase activity and SH2 domain regulate the dynamics of Src association with lipid and protein targets. J. Cell Biol. 178, 675–686.
50 Fincham, V. J., Unlu, M., Brunton, V. G., Pitts, J. D., Wyke, J. A. and Frame, M. C. (1996). Translocation of Src kinase to the cell periphery is mediated by the actin cytoskeleton under the control of the Rho family of small G proteins. J. Cell Biol. 135, 1551–1564.
51 Ridley, A. J., Paterson, H. F., Johnston, C. L., Diekmann, D. and Hall, A. (1992). The small GTP-binding protein rac regulates growth factor-induced membrane ruffling. Cell 70, 401–410.
52 Norman, J. C., Price, L. S., Ridley, A. J., Hall, A. and Koffer, A. (1994). Actin filament organization in activated mast cells is regulated by heterotrimeric and small GTP-binding proteins. J. Cell Biol. 126, 1005–1015.
53 Partridge, M. A. and Marcantonio, E. E. (2006). Initiation of attachment and generation of mature focal adhesions by integrin-containing filopodia in cell spreading. Mol. Biol. Cell. 17, 4237–4248.
54 Lu, S., Ouyang, M., Seong, J., Zhang, J., Chien, S. and Wang, Y. (2008). The spatiotemporal pattern of Src activation at lipid rafts revealed by diffusion-corrected FRET imaging. PLoS Comput. Biol. 4, e1000127.